Iwasaki, M., Miwa, S., Ikegami, T., Tomita, M., Tanaka, N., and Ishihama, Y. (2010). One-dimensional capillary liquid chromatographic separation coupled with tandem mass spectrometry unveils the Escherichia coli proteome on a microarray scale. Anal. Chem. *82*, 2616–2620.

Jørgensen, C., Sherman, A., Chen, G.I., Pasculescu, A., Poliakov, A., Hsiung, M., Larsen, B., Wilkinson, D.G., Linding, R., and Pawson, T. (2009). Cell-specific information processing in segregating populations of Eph receptor ephrin-expressing cells. Science *326*, 1502–1509.

Joughin, B.A., Liu, C., Lauffenburger, D.A., Hogue, C.W., and Yaffe, M.B. (2012). Protein kinases display minimal interpositional dependence on substrate sequence: potential implications for the evolution of signalling networks. Philos. Trans. R. Soc. Lond. B Biol. Sci. *367*, 2574–2583.

Joyce, A.R., and Palsson, B.O. (2006). The model organism as a system: integrating 'omics' data sets. Nat. Rev. Mol. Cell Biol. *7*, 198–210.

Kanehisa, M., Goto, S., Sato, Y., Furumichi, M., and Tanabe, M. (2012). KEGG for integration and interpretation of large-scale molecular data sets. Nucleic Acids Res. *40*, D109–D114.

Kubota, H., Noguchi, R., Toyoshima, Y., Ozaki, Y., Uda, S., Watanabe, K., Ogawa, W., and Kuroda, S. (2012). Temporal coding of insulin action through multiplexing of the AKT pathway. Mol. Cell *46*, 820–832.

Kühner, S., van Noort, V., Betts, M.J., Leo-Macias, A., Batisse, C., Rode, M., Yamada, T., Maier, T., Bader, S., Beltran-Alvarez, P., et al. (2009). Proteome organization in a genome-reduced bacterium. Science *326*, 1235–1240.

Li, C., Donizelli, M., Rodriguez, N., Dharuri, H., Endler, L., Chelliah, V., Li, L., He, E., Henry, A., Stefan, M.I., et al. (2010). BioModels Database: An enhanced, curated and annotated resource for published quantitative kinetic models. BMC Syst. Biol. *4*, 92.

Linding, R., Jensen, L.J., Ostheimer, G.J., van Vugt, M.A., Jørgensen, C., Miron, I.M., Diella, F., Colwill, K., Taylor, L., Elder, K., et al. (2007). Systematic discovery of in vivo phosphorylation networks. Cell *129*, 1415–1426.

Lindsay, J.R., McKillop, A.M., Mooney, M.H., Flatt, P.R., Bell, P.M., and O'harte, F.P. (2003). Meal-induced 24-hour profile of circulating glycated insulin in type 2 diabetic subjects measured by a novel radioimmunoassay. Metabolism *52*, 631–635.

Link, H., Kochanowski, K., and Sauer, U. (2013). Systematic identification of allosteric protein-metabolite interactions that control enzyme activity in vivo. Nat. Biotechnol. *31*, 357–361.

Locasale, J.W., Grassian, A.R., Melman, T., Lyssiotis, C.A., Mattaini, K.R., Bass, A.J., Heffron, G., Metallo, C.M., Muranen, T., Sharfi, H., et al. (2011). Phosphoglycerate dehydrogenase diverts glycolytic flux and contributes to oncogenesis. Nat. Genet. *43*, 869–874.

Lowery, D.M., Clauser, K.R., Hjerrild, M., Lim, D., Alexander, J., Kishi, K., Ong, S.E., Gammeltoft, S., Carr, S.A., and Yaffe, M.B. (2007). Proteomic screen defines the Polo-box domain interactome and identifies Rock2 as a Plk1 substrate. EMBO J. *26*, 2262–2273.

Miller, M.L., Jensen, L.J., Diella, F., Jørgensen, C., Tinti, M., Li, L., Hsiung, M., Parker, S.A., Bordeaux, J., Sicheritz-Ponten, T., et al. (2008). Linear motif atlas for phosphorylation-dependent signaling. Sci. Signal. *1*, ra2.

Monetti, M., Nagaraj, N., Sharma, K., and Mann, M. (2011). Large-scale phosphosite quantification in tissues by a spike-in SILAC method. Nat. Methods *8*, 655–658.

Mor, I., Cheung, E.C., and Vousden, K.H. (2011). Control of glycolysis through regulation of PFK1: old friends and recent additions. Cold Spring Harb. Symp. Quant. Biol. *76*, 211–216.

Nilsson, T., Mann, M., Aebersold, R., Yates, J.R., 3rd, Bairoch, A., and Bergeron, J.J. (2010). Mass spectrometry in high-throughput proteomics: ready for the big time. Nat. Methods *7*, 681–685.

Nimmo, H.G., and Tipton, K.F. (1975). The purification of fructose 1,6-diphosphatase from ox liver and its activation by ethylenediaminetetra-acetate. Biochem. J. *145*, 323–334.

Noguchi, R., Kubota, H., Yugi, K., Toyoshima, Y., Komori, Y., Soga, T., and Kuroda, S. (2013). The selective control of glycolysis, gluconeogenesis and glycogenesis by temporal insulin patterns. Mol. Syst. Biol. *9*, 664.

O'Connell, B.C., Adamson, B., Lydeard, J.R., Sowa, M.E., Ciccia, A., Bredemeyer, A.L., Schlabach, M., Gygi, S.P., Elledge, S.J., and Harper, J.W. (2010). A genome-wide camptothecin sensitivity screen identifies a mammalian MMS22L-NFKBIL2 complex required for genomic stability. Mol. Cell *40*, 645–657.

Oliveira, A.P., Ludwig, C., Picotti, P., Kogadeeva, M., Aebersold, R., and Sauer, U. (2012). Regulation of yeast central metabolism by enzyme phosphorylation. Mol. Syst. Biol. *8*, 623.

Olsen, J.V., Blagoev, B., Gnad, F., Macek, B., Kumar, C., Mortensen, P., and Mann, M. (2006). Global, in vivo, and site-specific phosphorylation dynamics in signaling networks. Cell *127*, 635–648.

Palsson, B. (2011). Systems biology: simulation of dynamic network states (Cambridge: Cambridge University Press).

Passonneau, J.V., and Lowry, O.H. (1963). P-Fructokinase and the control of the citric acid cycle. Biochem. Biophys. Res. Commun. *13*, 372–379.

Polonsky, K.S., Given, B.D., and Van Cauter, E. (1988). Twenty-four-hour profiles and pulsatile patterns of insulin secretion in normal and obese subjects. J. Clin. Invest. *81*, 442–448.

Rakus, D., Skalecki, K., and Dzugaj, A. (2000). Kinetic properties of pig (Sus scrofa domestica) and bovine (Bos taurus) D-fructose-1,6-bisphosphate 1-phosphohydrolase (F1,6BPase): liver-like isozymes in mammalian lung tissue. Comp. Biochem. Physiol. B Biochem. Mol. Biol. *127*, 123–134.

Rider, M.H., Bertrand, L., Vertommen, D., Michels, P.A., Rousseau, G.G., and Hue, L. (2004). 6-phosphofructo-2-kinase/fructose-2,6-bisphosphatase: head-to-head with a bifunctional enzyme that controls glycolysis. Biochem. J. *381*, 561–579.

Schomburg, I., Chang, A., Placzek, S., Söhngen, C., Rother, M., Lang, M., Munaretto, C., Ulas, S., Stelzer, M., Grote, A., et al. (2013). BRENDA in 2013: integrated reactions, kinetic data, enzyme function data, improved disease classification: new options and contents in BRENDA. Nucleic Acids Res. *41*, D764–D772.

Schöneberg, T., Kloos, M., Brüser, A., Kirchberger, J., and Sträter, N. (2013). Structure and allosteric regulation of eukaryotic 6-phosphofructokinases. Biol. Chem. *394*, 977–993.

Shyh-Chang, N., Locasale, J.W., Lyssiotis, C.A., Zheng, Y., Teo, R.Y., Ratanasirintrawoot, S., Zhang, J., Onder, T., Unternaehrer, J.J., Zhu, H., et al. (2013). Influence of threonine metabolism on S-adenosylmethionine and histone methylation. Science *339*, 222–226.

Simpson, C.J., and Fothergill-Gilmore, L.A. (1991). Isolation and sequence of a cDNA encoding human platelet phosphofructokinase. Biochem. Biophys. Res. Commun. *180*, 197–203.

Soga, T., Ueno, Y., Naraoka, H., Ohashi, Y., Tomita, M., and Nishioka, T. (2002). Simultaneous determination of anionic intermediates for Bacillus subtilis metabolic pathways by capillary electrophoresis electrospray ionization mass spectrometry. Anal. Chem. *74*, 2233–2239.

Vander Heiden, M.G., Locasale, J.W., Swanson, K.D., Sharfi, H., Heffron, G.J., Amador-Noguez, D., Christofk, H.R., Wagner, G., Rabinowitz, J.D., Asara, J.M., and Cantley, L.C. (2010). Evidence for an alternative glycolytic pathway in rapidly proliferating cells. Science *329*, 1492–1499.

Whiteman, E.L., Cho, H., and Birnbaum, M.J. (2002). Role of Akt/protein kinase B in metabolism. Trends Endocrinol. Metab. *13*, 444–451.

Wiley, H.S. (2011). Integrating multiple types of data for signaling research: challenges and opportunities. Sci. Signal. *4*, pe9.

Wittmann, C., Hans, M., van Winden, W.A., Ras, C., and Heijnen, J.J. (2005). Dynamics of intracellular metabolites of glycolysis and TCA cycle during cell-cycle-related oscillation in Saccharomyces cerevisiae. Biotechnol. Bioeng. *89*, 839–847.

Yus, E., Maier, T., Michalodimitrakis, K., van Noort, V., Yamada, T., Chen, W.H., Wodke, J.A., Güell, M., Martínez, S., Bourgeois, R., et al. (2009). Impact of genome reduction on bacterial metabolism and its regulation. Science *326*, 1263–1268.

Skp1-Cullin-F-box (SCF)-type ubiquitin ligase FBXW7 negatively regulates spermatogonial stem cell self-renewal

Mito Kanatsu-Shinohara[a,b,1], Ichiro Onoyama[c], Keiichi I. Nakayama[c,d], and Takashi Shinohara[a,d]

[a]Department of Molecular Genetics, Graduate School of Medicine, Kyoto University, Kyoto 606-8501, Japan; [b]Precursory Research for Embryonic Science and Technology (PRESTO) and [d]Core Research for Evolutionary Science and Technology (CREST), Japan Science and Technology Agency (JST), Tokyo 102-0076, Japan; and [c]Department of Molecular and Cellular Biology, Medical Institute of Bioregulation, Kyushu University, Fukuoka 812-8582, Japan

Edited by John J. Eppig, The Jackson Laboratory, Bar Harbor, ME, and approved May 7, 2014 (received for review January 31, 2014)

Spermatogonial stem cells (SSCs) undergo self-renewal divisions to support spermatogenesis throughout life. Although several positive regulators of SSC self-renewal have been discovered, little is known about the negative regulators. Here, we report that F-box and WD-40 domain protein 7 (FBXW7), a component of the Skp1-Cullin-F-box–type ubiquitin ligase, is a negative regulator of SSC self-renewal. FBXW7 is expressed in undifferentiated spermatogonia in a cell cycle-dependent manner. Although peptidyl-prolyl cis/trans isomerase NIMA-interacting 1 (PIN1), essential for spermatogenesis, is thought to destroy FBXW7, *Pin1* depletion decreased FBXW7 expression. Spermatogonial transplantation showed that *Fbxw7* overexpression compromised SSC activity whereas *Fbxw7* deficiency enhanced SSC colonization and caused accumulation of undifferentiated spermatogonia, suggesting that the level of FBXW7 is critical for self-renewal and differentiation. Screening of putative FBXW7 targets revealed that *Fbxw7* deficiency up-regulated myelocytomatosis oncogene (MYC) and cyclin E1 (CCNE1). Although depletion of *Myc*/*Mycn* or *Ccne1*/*Ccne2* compromised SSC activity, overexpression of *Myc*, but not *Ccne1*, increased colonization of SSCs. These results suggest that FBXW7 regulates SSC self-renewal in a negative manner by degradation of MYC.

Spermatogonial stem cells (SSCs) provide the foundation for spermatogenesis by undergoing self-renewing division (1, 2). SSCs reside in a special niche microenvironment where they are provided with self-renewal factors that stimulate proliferation. Glial cell line-derived neurotrophic factor (GDNF) is secreted from the niche to promote SSC self-renewal (3). Studies on SSCs are hampered because SSCs constitute only 0.02–0.03% of germ cells, which amounts to 2–3 $\times$ 10^4 cells per mouse testis (2, 4). Moreover, the lack of a specific marker has made it difficult to distinguish SSCs from committed spermatogonia. In 1994, a germ cell transplantation technique was developed (5), in which transplanted SSCs reinitiate spermatogenesis and produce functional sperm following microinjection into seminiferous tubules of testes. Moreover, the addition of GDNF stimulated self-renewing division of SSCs and allowed long-term expansion in vitro. Cultured cells, designated as germ-line stem (GS) cells, proliferate for at least 2 y and expand to 10^{85}-fold, creating a unique opportunity to collect a large number of SSCs for biochemical and molecular biological analyses (6).

Using these techniques, molecular regulators of SSC self-renewal have been analyzed. It is now considered that GDNF activates Harvey rat sarcoma virus oncogene (HRAS) via *Src* family kinase molecules, and cells transfected with activated HRAS underwent self-renewal division without exogenous cytokines (7). Chemical inhibition of thymoma viral proto-oncogene (AKT) or mitogen-activated protein kinase kinase 1 (MAP2K1), both of which are downstream molecules of HRAS, abrogated GS cell proliferation (8–10), suggesting that they are necessary for self-renewal division. When active *Akt* or *Map2k1* was overexpressed in GS cells, *Akt*- or *Map2k1*-transfected cells could proliferate with only fibroblast growth factor 2 (FGF2) or GDNF, respectively (8, 9). These signals up-regulate *Etv5* and *Bcl6b* (8, 11), which work in combination with other constitutively expressed transcription factors, such as zinc finger and BTB domain containing 16 (*Zbtb16*) or *Taf4b*, to drive SSC self-renewal.

Although these studies have identified several positive regulators of SSC self-renewal, little is known about the negative regulators, which would be equally important in understanding stem-cell kinetics. In this study, we analyzed the function of the F-box protein FBXW7 (also known as *Fbw7*, *Cdc4*, *Fbxw6*, or *Fbxo30*), a substrate recognition subunit of the Skp1-Cullin-F-box complex (12). FBXW7 catalyzes the ubiquitination of various molecules involved in cell-fate decision and cell-cycle regulation. We hypothesized that degradation of these critical regulators by FBXW7 influences cell-cycle regulation or fate commitment in SSCs. We tested this hypothesis by taking advantage of SSC cultures and transplantation techniques.

Results

Restricted Expression of FBXW7 in Spermatogonia. We examined FBXW7 expression in seminiferous tubules of 1-, 10-, and 42-d-old mice (Fig. S1 *A–D*). In 1-d-old testes, FBXW7 was expressed in most of the gonocytes, which are precursors of spermatogonia. However, FBXW7 expression was significantly decreased in 10-d-old mouse testes, which contain proliferating spermatogonia. All stages of germ cells are present in 42-d-old testes, but

Significance

Spermatogonial stem cells (SSCs) are at the foundation of spermatogenesis. Previous studies on SSC self-renewal have focused on the positive regulation, but we hypothesized that negative regulation of self-renewal is equally important in understanding SSC self-renewal. We show here that F-box and WD-40 domain protein 7 (FBXW7), a component of the Skp1-Cullin-F-box–type ubiquitin ligase, negatively regulates SSC self-renewal. FBXW7 is expressed only in the undifferentiated spermatogonia compartment, and its overexpression compromises SSC activity whereas *Fbxw7* deficiency enhances SSC colonization and caused accumulation of undifferentiated spermatogonia. We also demonstrate that FBXW7 regulates stability of myelocytomatosis oncogene (MYC), which increased SSC activity upon overexpression. These results suggest that FBXW7 counteracts with positive regulators of self-renewal by degrading MYC and demonstrate the importance of negative regulators of self-renewal in understanding SSC homeostasis.

Author contributions: M.K.-S. designed research; M.K.-S. and T.S. performed research; M.K.-S., I.O., and K.I.N. contributed new reagents/analytic tools; M.K.-S. and T.S. analyzed data; and M.K.-S. and T.S. wrote the paper.

The authors declare no conflict of interest.

This article is a PNAS Direct Submission.

[1]To whom correspondence should be addressed. E-mail: mshinoha@virus.kyoto-u.ac.jp.

This article contains supporting information online at www.pnas.org/lookup/suppl/doi:10.1073/pnas.1401837111/-/DCSupplemental.

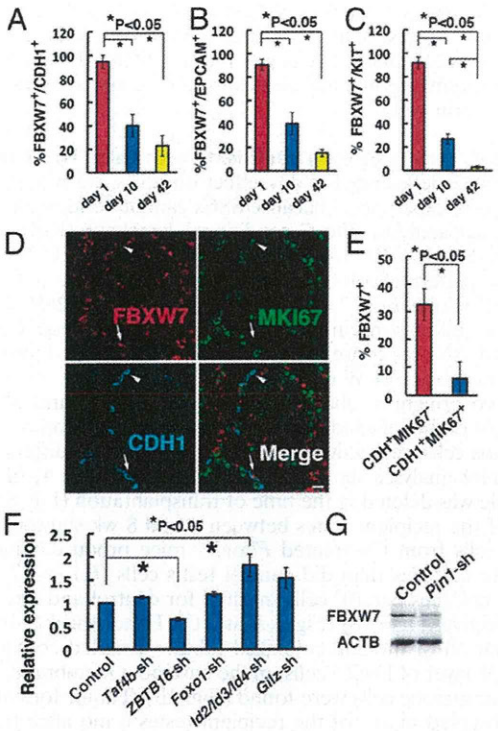

Fig. 1. Expression of FBXW7 in spermatogonia. (*A–C*) Expression of FBXW7 protein in CDH1$^+$ (*A*), EPCAM$^+$ (*B*), or KIT$^+$ (*C*) cells during postnatal testis development. At least 12, 15, and 14 tubules were counted in 1-, 10-, and 42-d-old testes, respectively. (*D*) Triple immunohistochemistry of FBXW7, MKI67, and CDH1 in 42-d-old testes. At least 17 tubules were counted. Arrows indicate CDH1$^+$MKI67$^-$ cells with FBXW7 expression. Arrowheads indicate CDH1$^+$ MKI67$^+$ cells without FBXW7 expression. (*E*) Proportion of CDH1$^+$ cells with FBXW7 expression. (*F*) Real-time PCR analysis of *Fbxw7* expression following depletion of indicated genes by shRNA ($n = 6$). (*G*) Western blot analysis of FBXW7 expression following *Pin1* depletion. (Scale bar: *D*, 20 μm.)

FBXW7 was found in only 22.7% of cadherin 1 (CDH1)-expressing undifferentiated spermatogonia and 15.1% of epitherial cell adhesion molecule (EPCAM)-expressing spermatogonia (Fig. 1 *A* and *B* and Table S1). FBXW7 was rarely found in kit oncogene (KIT)-expressing differentiating spermatogonia of adult testes (Fig. 1*C*). These results suggested that FBXW7 is expressed during the primitive stages of spermatogenesis but down-regulated during differentiation. Interestingly, FBXW7 expression was more frequently found in CDH1$^+$ antigen identified by monoclonal antibody Ki67 (MKI67)$^-$ spermatogonia compared with CDH1$^+$ MKI67$^+$spermatogonia (Fig. 1 *D* and *E*), which suggests that FBXW7 is expressed in a cell cycle-specific manner.

To examine the regulation of *Fbxw7*, we used GS cells and enriched germ cells from pup testis. Self-renewal factors, including FGF2 and GDNF, did not show an apparent effect (Fig. S2 *A* and *B*). GDNF also did not induce apparent changes in pup testis cells after gelatin selection, which are enriched for SSCs (Fig. S2 *C* and *D*). Screening of *Fbxw7* regulators using lentiviruses expressing short hairpin RNA (shRNA) revealed that depletion of *Zbtb16* reduced the expression of *Fbxw7* whereas depletion of inhibitor of DNA binding (*Id*)*2/3/4* increased *Fbxw7* mRNA expression (Fig. 1*F*, Fig. S2*E*, and Table S2). However, Western blotting showed no significant changes after these treatments (Fig. S2*F*). Nevertheless, because several F-box proteins, including FBXW7, are unstable and regulated posttranslationally (13), we also analyzed the impact of *Pin1*, a prolyl isomerase that was reported to change FBXW7 protein expression: *Pin1* overexpression down-regulated FBXW7 whereas its depletion led to elevated FBXW7 expression in human cancer cells (14). Contrary to our expectation, *Pin1* depletion down-regulated FBXW7 expression (Fig. 1*G* and Fig. S2 *E* and *G*). In contrast, *Pin1* overexpression did not influence FBXW7 expression (Fig. S2 *H* and *I*), suggesting that PIN1 is necessary but not sufficient for maintaining FBXW7 expression.

Overexpression of Fbxw7 Suppresses the Proliferation of SSCs. There are three isoforms of *Fbxw7* (*Fbxw7α*, -β, and -γ), and reverse-transcriptase (RT)-PCR analysis showed that *Fbxw7α* was strongly expressed in GS cells (Fig. 2*A*). To examine the impact of *Fbxw7α* overexpression in SSCs, lentivirus-mediated transduction of *Fbxw7α* and *Venus* was performed in testis cells from 10-d-old C57BL/6 Tg14(act-EGFP)OsbY01 (green) transgenic mice that ubiquitously express enhanced green fluorescent protein (EGFP). After overnight infection, the viral supernatant was removed, and, after 2 d, *Fbxw7α*-transduced cells were transplanted into seminiferous tubules of WBB6F1-W/W^v (W) mice. Testis cells transduced with an *Fbxw7α*-expressing vector produced 3.3 ± 0.8 colonies per 10^5 cells whereas control testis cells produced 9.2 ± 1.0 colonies per 10^5 cells ($n = 12$), and this decrease in colony number was statistically significant (Fig. 2*B* and Fig. S3*A*).

To understand the mechanism mediating the decrease in SSC induced by *Fbxw7α* overexpression, we performed transfection experiments using GS cells from B6-TgR(ROSA26)26Sor (ROSA26) mice. Flow cytometry analysis showed that *Fbxw7α* overexpression conferred a selective disadvantage for GS cell proliferation (Fig. 2 *C* and *D*). Although the proportion of cells displaying Venus fluorescence was comparable 4 d after infection, it dropped significantly after 15 d. Consistent with this observation, cell recovery was also decreased by *Fbxw7α* transfection, which suggested that *Fbxw7α* overexpression suppresses GS cell proliferation (Fig. 2*E*). This growth suppression occurred despite decreased expression of several cyclin-dependent kinase inhibitors (CDKIs) (Fig. S3*B*). Adding GDNF did not influence colonization levels of primary pup testis cells (Fig. S3*C*). Taken together, these results suggest that *Fbxw7α* overexpression has a negative impact on SSC self-renewal.

Conditional Deletion of Fbxw7 Impairs Spermatogenesis. To examine the impact of *Fbxw7* deletion on spermatogenesis, we crossed mice homozygous for the floxed *Fbxw7* allele (*Fbxw7*$^{f/f}$) with stimulated by retinoic acid gene 8 (*Stra8*)-*Cre* transgenic mice, which express *Cre* recombinase under the *Stra8*-promoter (15).

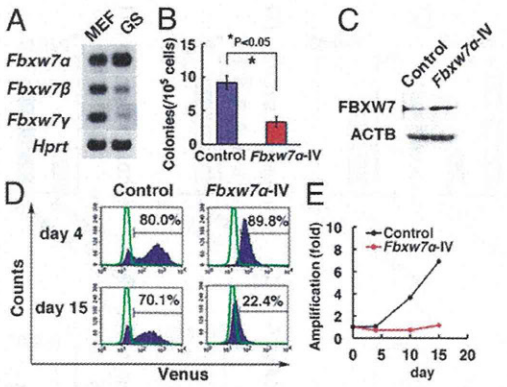

Fig. 2. Decreased SSC activity with *Fbxw7* overexpression. (*A*) RT-PCR analysis of *Fbxw7* isoform expression in GS cells and mouse embryonic fibroblasts (MEFs). (*B*) Colony counts after *Fbxw7α* overexpression and transplantation of green mouse testis cells. Results of two experiments ($n = 12$). (*C*) Western blot analysis of *Fbxw7α* expression in GS cells transduced with *Fbxw7α*. Cells were recovered 4 d after transfection. (*D*) Flow cytometric analysis of GS cells transduced with *Fbxw7α*. Cells were analyzed at the indicated time points. Green lines indicate GS cells without transfection. (*E*) Proliferation of GS cells following *Fbxw7α* overexpression.

CELL BIOLOGY

Stra8 is a retinoic acid-responsive gene, which is first expressed a few days after birth in the majority of ZBTB16$^+$ undifferentiated spermatogonia. Testes of *Fbxw7*$^{f/f}$ *Stra8-Cre* adult mice were apparently smaller than those of controls (*Fbxw7*$^{+/+}$ *Stra8-Cre*) (Fig. 3*A*). Histological analysis of 2-mo-old *Fbxw7*$^{f/f}$ *Stra8-Cre* testes revealed significantly reduced germ cells in mutant testes, and few meiotic cells were found (Fig. 3*B*). The number of tubules with spermatogenesis, as defined by the tubules with multiple layers of germ cells, was significantly decreased by *Fbxw7* deficiency (Fig. 3*C*).

Double immunohistochemistry of the testes showed that the frequency of FBXW7-expressing cells in CDH1$^+$ spermatogonia was reduced from 20.1% in the control to 3.2% in *Fbxw7*$^{f/f}$ *Stra8-Cre* mice, suggesting that the deletion efficiency was 84.1% (Fig. 3*D* and Fig. S4*A*). We also found that expression of synaptonemal complex protein 3 (SYCP3), a marker for meiotic germ cells, was significantly suppressed in these mice (Fig. 3*E* and Fig. S4*B*). On the other hand, the seminiferous tubules of *Fbxw7*$^{f/f}$ *Stra8-Cre* mice contained a high number of CDH1$^+$ spermatogonia per Sertoli cells, as evaluated by the ratio of CDH1$^+$ to GATA binding protein 4 (GATA4)$^+$ Sertoli cells (Fig. 3*F* and Fig. S4*C*). Similar results are found for KIT (Fig. 3*G* and Fig. S4*D*), suggesting that FBXW7 plays a role in restricting the proliferation of spermatogonia. Terminal deoxynucleotidyl transferase dUTP nick end labeling (TUNEL) staining showed increased apoptosis in EPCAM$^+$ cells, but not in KIT$^+$ cells (Fig. 3 *H–J* and Fig. S4 *E* and *F*). Because EPCAM is expressed on spermatogonia and KIT is expressed on germ cells up to the pachytene stage, this observation suggests that spermatogonia are predominantly undergoing apoptosis. We also observed a greater frequency of MKI67$^+$ cells in both CDH1- and KIT-expressing spermatogonia in *Fbxw7*$^{f/f}$ *Stra8-Cre* mice (Fig. 3 *K* and *L* and Fig. S4 *G* and *H*). These results suggest that, in *Fbxw7*$^{f/f}$ *Stra8-Cre* mice, *Fbxw7* deletion not only induces the proliferation of CDH1- and KIT-expressing spermatogonia but also causes increased apoptosis of premeiotic germ cells.

Enhanced SSC Activity of Fbxw7-Deficient Testis Cells. To examine whether *Fbxw7* deficiency has any effect on SSCs, we performed transplantation experiments because SSCs cannot be identified by morphological analysis. *Fbxw7* conditional knockout (KO) mice were crossed with a ROSA26 reporter mouse strain (R26R) to visualize the pattern of colonization (16). Testis cells were collected from 8- to 11-d-old *Fbxw7*$^{f/f}$ mice heterozygous for the R26R allele, and a single-cell suspension was exposed to a *Cre*-expressing adenovirus (AxCANCre) overnight in vitro and then injected into the seminiferous tubules of W mice (Fig. 4*A* and Fig. S5*A*).

After an overnight incubation, 87.7 ± 7.1% (n = 4) and 84.3 ± 6.9% (n = 6) of the infected cells were recovered from control and mutant testis cells, respectively, showing no significant difference. Southern blot analyses showed that 63.6 ± 2.0% (n = 4) of the floxed allele was deleted at the time of transplantation (Fig. S5*B*). Analysis of the recipient testes between 6 and 8 wk showed that the testis cells from *Cre*-treated *Fbxw7*$^{f/f}$ mice produced significantly more colonies than did control testis cells (6.1 ± 1.7 and 15.3 ± 3.2 colonies per 10^5 cells injected for control and *Fbxw7*$^{f/f}$ mice, respectively; n = 18) (Fig. 4 *B* and *C*). Histological analyses showed that all of the 282 colonized tubules counted contained only a single layer of LacZ$^+$ cells on the basement membrane, and no apparent meiotic cells were found (Fig. 4*B*). Tumor formation was not observed in any of the recipient testes 6 mo after transplantation (n = 8). RT-PCR analysis of recipient testes showed

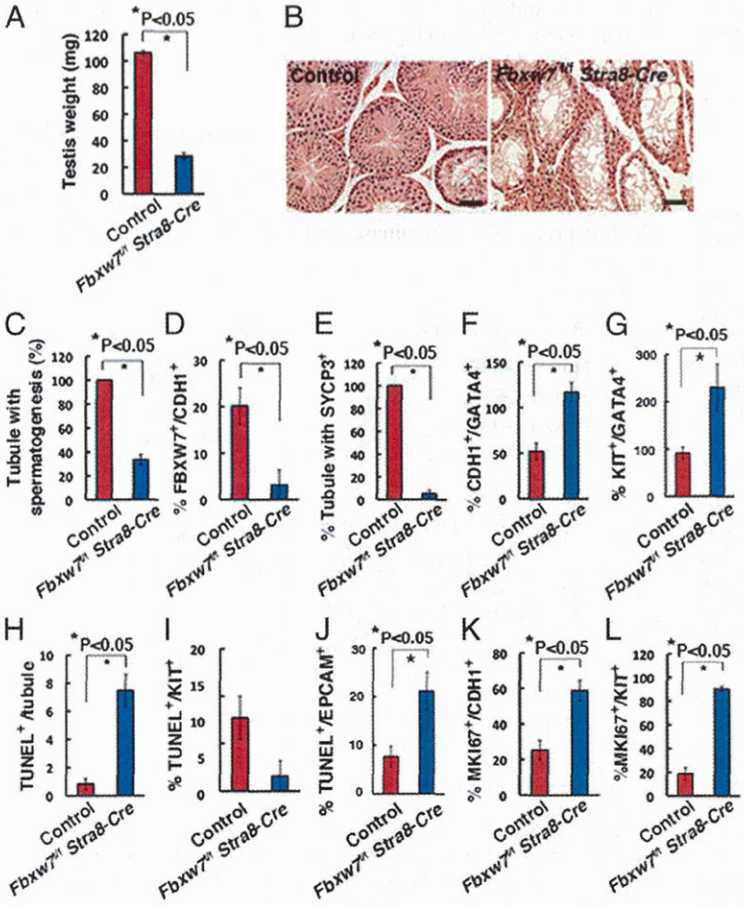

Fig. 3. Impaired spermatogenesis in *Fbxw7*$^{f/f}$ *Stra8-Cre* mice. (*A*) Testis weight of 2-mo-old *Fbxw7*$^{f/f}$ *Stra8-Cre* mice (n = 8, control; n = 6, *Fbxw7*$^{f/f}$ *Stra8-Cre*). (*B*) Histological appearance of *Fbxw7*$^{f/f}$ *Stra8-Cre* testis. (*C*) Tubules with spermatogenesis, defined as the presence of multiple layers of germ cells in the entire circumference of the tubules. At least 207 tubules were counted. (*D*) Expression of FBXW7 in CDH1$^+$ cells. At least 20 tubules were counted. (*E*) Expression of SYCP3 in KIT$^+$ cells. At least 22 tubules were counted. (*F*) Ratio of CDH1$^+$ spermatogonia and GATA4$^+$ Sertoli cells. At least 34 tubules were counted. (*G*) Ratio of KIT$^+$ spermatogonia and GATA4$^+$ Sertoli cells. At least 8 tubules were counted. (*H*) The number of TUNEL$^+$ cells in seminiferous tubules. At least 11 tubules were counted. (*I*) The number of KIT$^+$ cells undergoing apoptosis. At least 8 tubules were counted. (*J*) The number of EPCAM$^+$ cells undergoing apoptosis. At least 10 tubules were counted. (*K*) Expression of MKI67 in CDH1$^+$ cells. Eighteen tubules were counted. (*L*) Expression of MKI67 protein in KIT$^+$ cells. Twenty tubules were counted. (Scale bar: *B*, 50 μm.) Stain, hematoxylin/eosin (*B*).

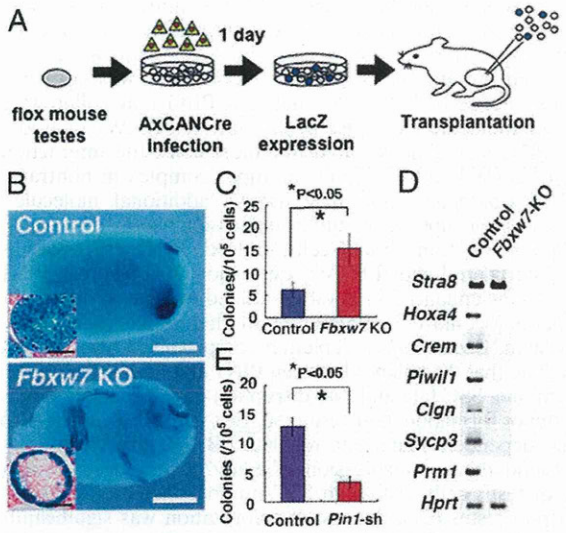

Fig. 4. Enhanced SSC activity in *Fbxw7* KO testis cells. (*A*) Experimental procedure. Testis cells from *Fbxw7*$^{f/f}$ mice were dissociated and incubated with AxCANCre overnight and then injected into the seminiferous tubules of W testes. (*B*) Macroscopic appearance of recipient testis. Histological appearance (*Inset*). (*C*) Colony counts after *Cre* transfection and transplantation of *Fbxw7*$^{f/f}$ mouse testes. Results of three experiments (n = 18). (*D*) RT-PCR analysis of spermatogenic gene expression in recipient testes. (*E*) Colony counts after *Pin1* depletion and transplantation of green mouse testes. Results of two experiments (n = 16). (Scale bars: *B*, 1 mm; *B*, *Inset*, 50 μm.)

that expression of meiotic germ cell markers, such as *Hoxa4* and *Sycp3*, was significantly reduced or not detected (Fig. 4*D*).

Although *Fbxw7* deficiency increased the concentration of SSCs, this result appeared to contradict a previous observation that *Pin1* deficiency induced spermatogonia depletion (17), given that *Pin1* depletion caused a decrease in FBXW7 level. Because PIN1 is also expressed in Sertoli cells and may influence spermatogenesis, we directly examined the impact of *Pin1* depletion in germ cells by spermatogonial transplantation. We transduced testis cells from 9-d-old green mouse pups with shRNA against *Pin1*, and the cells were transplanted into W mice 2 d later. Analysis of the recipient mice showed significantly reduced colonies with *Pin1* depletion (Fig. 4*E*). The number of colonies generated by cells transduced with control and *Pin1* shRNA was 12.9 ± 1.5 and 3.3 ± 1.0 per 10^5 cells (n = 16). This result suggests that PIN1 expression in germ cells is essential for SSC activity and that PIN1 has additional targets involved in self-renewal.

Screening of Fbxw7 Target Proteins Using GS Cells. To investigate the molecular machinery involved in FBXW7-mediated self-renewal regulation, *Fbxw7*$^{f/f}$ GS cells were established and exposed in vitro to AxCANCre overnight. Unlike the deletion of primary testis cells, Southern blot analyses showed that the floxed allele was completely deleted from the *Fbxw7* gene locus, which likely reflected enhanced proliferation of the *Fbxw7* KO population (Fig. S6*A*). Consistent with this observation, the amplification rate was increased significantly after *Cre*-mediated deletion of *Fbxw7* gene (Fig. 5*A*), which was supported by the increased frequency of MKI67$^+$ cells in mutant cells (Fig. 5*B* and Fig. S6*B*). Flow cytometric analysis showed no significant changes in the expression of known spermatogonia markers (Fig. S6*C*).

To investigate molecules involved in enhanced spermatogonial proliferation, we first examined the expression of molecules involved in cell proliferation using *Fbxw7* KO GS cells (Fig. S6*D*). We found not only increased expression of CCND1, phosphorylated MAPK14 (p-MAPK14), and AKT (p-AKT), but also decreased expression of cyclin-dependent kinase inhibitor 2B (CDKN2B) (Fig. 5*C*). We then analyzed the expression of candidate substrates of FBXW7. The expression of neither NOTCH1 nor NOTCH2 was enhanced by *Fbxw7* deficiency (Fig. S6*E*). Levels of NICD (Notch intracellular domain) did not show significant changes (Fig. S6*F*). Moreover, adding a γ-secretase inhibitor *N*-[*N*-(3,5-difluorophenacetyl)-L-alanyl]-S-phenylglycine t-butyl ester (DAPT) or depletion of *Rbpj*, the common DNA binding partner of all Notch receptors, by shRNA did not influence proliferation of *Fbxw7* KO GS cells (Fig. S6 *G–I*). We also checked several NOTCH target genes by real-time PCR. Although *Hes1* expression was slightly increased, the rest of the genes did not change significantly by *Fbxw7* deficiency (Fig. S6*J*). In contrast, expression of myelocytomatosis oncogene (MYC) and cyclin E1 (CCNE1) was enhanced in *Fbxw7* KO GS cells (Fig. 5*D* and Fig. S6*K*). The expression levels of phosphorylated JUN (p-JUN), v-myc myelocytomatosis viral related oncogene, neuroblastoma derived (MYCN), SREBF1, MCL1, and KLF5 did not change significantly (Fig. 5*D* and Fig. S6*K*). We also did not detect changes in MTOR level, which reportedly influenced the expression of GDNF receptor components (18). These results suggest that MYC and CCNE1 are responsible for enhanced self-renewal of SSCs.

Myc Is Responsible for Enhanced SSC Activity by Fbxw7 Deficiency. Consistent with these observations, double immunohistochemistry revealed significantly enhanced expression of MYC and CCNE1 in CDH1$^+$ undifferentiated spermatogonia in *Fbxw7*$^{f/f}$ *Stra8-Cre* mice (Fig. 5 *E* and *F* and Fig. S7 *A* and *B*). When we examined several *Myc* classic target genes, we noted increased CDK4 expression in *Fbxw7*$^{f/f}$ *Stra8-Cre* mice (Fig. 5*G* and Fig. S7 *C–E*). To examine whether the accumulation of MYC and/or CCNE1 caused enhanced colonization after *Fbxw7* deletion, we investigated the effect of *Myc*/*Mycn* knockdown (KD) using *Fbxw7* KO mice. We used *Mycn* and *Ccne2* shRNA because loss of *Myc* or *Ccne1* may be compensated by these treatments (19, 20). Testis cells from 7-d-old *Fbxw7*$^{f/f}$ R26R mice were transduced with lentivirus expressing shRNA for *Myc*/*Mycn* or *Ccne1*/*Ccne2* by overnight incubation, followed by treatment with AxCANCre 2 d after lentiviral infection. After overnight incubation with AxCANCre, cells were injected into W testes (Fig. 5*H*). Colonization was significantly suppressed by either *Myc*/*Mycn* or *Ccne1*/*Ccne2* KD (Fig. 5*I* and Fig. S7*F*), suggesting positive roles for these molecules in SSC self-renewal.

Finally, we examined the impact of target gene overexpression. Testis cells from 8-d-old green mice were transduced with a lentivirus expressing *Myc*, *Mycn*, or *Ccne1*. After overnight infection, the viral supernatant was removed, and the cells were transplanted into seminiferous tubules of W mice the following day. Analysis of the recipient mice showed enhanced colonization of donor cells transduced with *Myc* or *Mycn*. In contrast, *Ccne1* overexpression did not affect colonization (Fig. 5*J* and Fig. S7*G*). *Myc* overexpression could also increase colonization of pup testis transduced with *Fbxw7* (Fig. S7*H*). Although *Pin1* depletion did not change MYC in GS cells, it significantly enhanced CCNE1 (Fig. S7 *I* and *J*). *Myc* silencing in *Pin1*-depleted cells did not induce significant changes in SSC activity (Fig. S7*K*). Because *Pin1* depletion decreased SSC activity (Fig. 4*E*), these results suggest that MYC mediates the enhanced SSC activity seen with *Fbxw7* deficiency.

Discussion

Recent studies revealed that *Fbxw7* plays pivotal roles in the regulation of several stem cells/progenitors (21–25). Most of the phenotypes of *Fbxw7* deficiency are related to cell proliferation, death, or skewed differentiation. However, effects on stem cell self-renewal are not always evident and can be variable. In testes, FBXW7 expression is restricted to a subset of spermatogonia in a cell cycle-specific manner. *Fbxw7* mRNA expression was down-regulated by *Zbtb16* depletion whereas it was up-regulated by *Id2*/*Id3*/*Id4* depletion. Increased *Fbxw7* expression by *Id2*/*Id3*/*Id4* depletion was intriguing. Given that ID proteins often influence cell-cycle progression (26), it is possible that ID proteins may

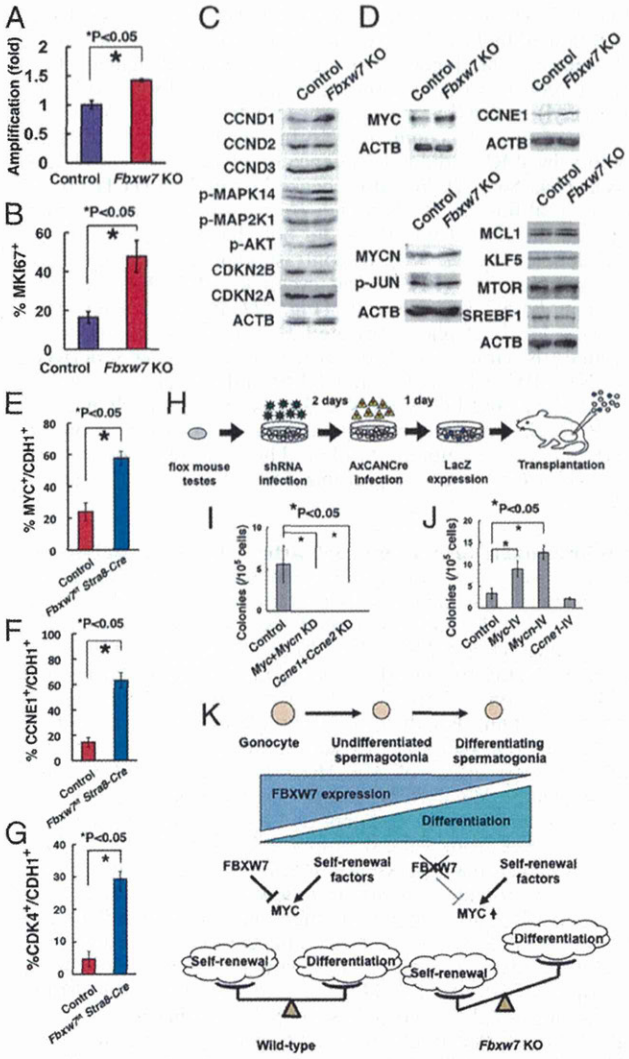

Fig. 5. Characterization of *Fbxw7* KO GS cells for target identification. (*A*) Enhanced proliferation of GS cells after *Cre* transfection. After overnight incubation with AxCANCre, virus supernatant was removed, and cells were replated in a new dish. Cell number was determined 3 d after replating. AxCANLacZ was used as a control (n = 4). Results of two experiments. (*B*) Quantification of GS cells expressing MKI67. At least 732 cells in four different fields were counted. (*C*) Western blot analysis of molecules involved in proliferation of GS cells. (*D*) Western blot analysis of FBXW7 substrates. (*E*) Expression of MYC in CDH1$^+$ cells in *Fbxw7$^{f/f}$ Stra8-Cre* testes. Fifteen tubules were counted. (*F*) Expression of CCNE1 in CDH1$^+$ cells in *Fbxw7$^{f/f}$ Stra8-Cre* testes. Fifteen tubules were counted. (*G*) Expression of CDK4 in CDH1 cells in *Fbxw7$^{f/f}$ Stra8-Cre* testes. At least 8 tubules were counted. (*H*) Experimental procedure. Immature testis cells from *Fbxw7$^{f/f}$* mice were infected with lentiviruses expressing shRNA against *Myc*/*Mycn* or *Ccne1*/*Ccne2*. Culture medium was changed on the next day after infection. Two days after shRNA infection, cells were infected with AxCANCre and transplanted 24 h after AxCANCre infection. (*I*) Colony counts after depleting the indicated genes (n = 8). Results of two experiments. (*J*) Colony counts after overexpression of indicated genes and transplantation of green mouse testis cells. Results of two experiments (n = 12). (*K*) Summary of experiments. Loss of FBXW7 increases self-renewal by up-regulation of MYC and suppresses differentiation.

play a role in regulating FBXW7 expression, which occurred in a cell cycle-dependent manner. However, depletion of these molecules did not lead to apparent changes in Western blots. Our screening further revealed that FBXW7 down-regulation occurs upon depletion of *Pin1*, whose deficiency causes male infertility (17). This result was unexpected because PIN1 is thought to promote FBXW7 degradation by causing self-ubiquitination (14). Although *Pin1* overexpression did not change FBXW7 expression, it is possible that the amount of PIN1 overexpression was not sufficient to influence FBXW7. Alternatively, PIN1 may collaborate with other molecules. Because promotion of FBXW7 degradation by PIN1 was demonstrated in cancer cells, the interaction between FBXW7 and PIN1 may be more complex in nontransformed spermatogonia and may involve additional molecules. *Fbxw7* is a tumor suppressor, and its expression needs to be tightly controlled in nontransformed cells. Indeed, PIN1 expression is inversely correlated with FBXW7 expression (14) whereas PIN1 expression was enhanced in undifferentiated relative to differentiating spermatogonia (17), suggesting another sophisticated regulation system. Because *Pin1* depletion compromised SSC activity, we speculate that the balance between PIN1 and FBXW7 is critical in determining SSC fate and that disruption of this regulation may induce tumor formation. Our results suggest that PIN1 functions in a context-dependent manner to regulate FBXW7 expression.

We found that overexpression of *Fbxw7α* compromised SSC activity of testis cells. Although SSC number increased dramatically in pup testes (27), donor-cell colonization was significantly decreased by *Fbxw7α* overexpression. Given the strong growth suppression of GS cells by *Fbxw7α* overexpression and its cell cycle-specific expression, this result suggests that the amount and timing of FBXW7 need to be tightly controlled to promote cell-cycle progression. It also suggests that committed progenitors proliferate faster than undifferentiated spermatogonia because they lack FBXW7 expression. However, we currently cannot explain why *Fbxw7α* overexpression reduced the colonization activity of SSCs. It might be related to the fact that FBXW7 is restricted to undifferentiated spermatogonia in the spermatogenic system. One possibility is that *Fbxw7α* -overexpressing SSCs may have seeded in the recipient testes but ectopic *Fbxw7α* overexpression in progenitors may have hindered colony formation. It is also possible that SSCs may have failed to colonize the recipient tubules due to cell-cycle dysregulation, which is one of the important factors involved in migration of SSCs to niches (28).

Our results showed that *Fbxw7* deletion increased proliferation of undifferentiated spermatogonia. Importantly, transplantation experiments confirmed its effect on SSCs. Together with the results from *Fbxw7* overexpression experiments, these results demonstrate that FBXW7 plays an important role in negatively regulating self-renewal. To our knowledge, this is the first report of increased SSC activity in KO mice. Although enhanced spermatogonial proliferation was observed in *Cdkn1b* KO mice (29), *Cdkn1b* is different from *Fbxw7* in that its deficiency promoted differentiating division and a decreased rather than increased SSC frequency. *Tsc22d3* deficiency was also associated with increased spermatogonia proliferation, but undifferentiated spermatogonia were lost in the adult (30). Mutations in other genes, such as *Sohlh1*/*Sohlh2*, suppressed differentiation (31), but *Fbxw7* is unique because its deficiency not only caused enhanced proliferation of undifferentiated spermatogonia but also increased self-renewal division. In this regard, it should be noted here that enhancement of self-renewal activity was accompanied by impaired differentiation and increased apoptosis. Although *Fbxw7* deficiency often caused apoptosis and skewed differentiation, complete suppression of differentiation has not been observed in other self-renewing tissues. In this sense, the spermatogenic system appears to be extremely sensitive to the amount of FBXW7 in differentiation.

In our search for candidate FBXW7 target molecules, we found up-regulation of MYC and CCNE1 in *Fbxw7* KO GS cells. *Myc* plays a key role in exit from and reentry into the cell cycle, and its overexpression was also implicated in human tumorigenesis (32). The function of *Mycn* in spermatogonia was reported in a previous study (33), which showed that *Mycn* is up-regulated by GDNF in a phosphatidylinositol 3-kinase-AKT dependent manner to contribute to proliferation. However, because this study was carried out in an SV40-transformed spermatogonia

cell line, the role of *Myc* family genes in SSCs has remained unclear. The importance of *Ccne1* in spermatogonia was demonstrated in several studies. *Ccne1* overexpression increased SSC self-renewal by cooperating with *Ccnd2* (7) whereas *Ccne2* deficiency compromised spermatogenesis (19).

Several lines of evidence suggest that MYC is a target substrate of FBXW7 in SSCs and that it increases SSC activity. First, loss of *Fbxw7* induced accumulation of MYC in undifferentiated spermatogonia and GS cells. Second, suppression of *Myc/Mycn* by shRNAs abolished the up-regulated SSC activity caused by *Fbxw7* deficiency. Third, *Myc* or *Mycn* overexpression increased the colonization efficiency of wild-type (WT) testis cells. Although depletion of *Ccne1* and *Ccne2* expression could reduce SSC activity, *Ccne1* overexpression did not enhance colonization, suggesting that CCNE1/CCNE2 are not involved in the abnormal phenotype of *Fbxw7* KO mice. Enhanced apoptosis in *Fbxw7*-deficient testis may also be caused by increased MYC expression (32). Taken together, these lines of evidence strongly suggest that FBXW7 counteracts with positive regulators of self-renewal by degrading MYC (Fig. 5*K*).

Although the current study identified a role for FBXW7 as a negative regulator of SSC self-renewal, several questions persist. For example, although PIN1 is thought to bind to FBXW7 in a phosphorylation-dependent manner, we need to find targets for PIN1 and whether they have any interaction with FBXW7. We also do not know why FBXW7 influenced the expression of MYC, but not MYCN, and whether MYC up-regulation is involved in the suppression of spermatogonial differentiation. Having identified, to our knowledge, the first negative regulator of SSCs, we are now at the stage to find other negative regulators that may counteract with self-renewal signals at different levels. In addition, modulation of FBXW7 function by small molecules may be useful for enhancement of SSC self-renewal in vitro for genetic modifications. Thus, identification of the negative regulator for SSC self-renewal not only deepens our knowledge of SSC biology but also adds a new dimension of investigation and possibilities.

Materials and Methods

Animals. The generation of *Fbxw7*$^{f/f}$ mice was described previously (34). WT C57BL/6 mice were purchased from Japan SLC. We also used 8- to 10-d-old green mice that ubiquitously express EGFP (a gift from D. M. Okabe, Osaka University, Osaka). Male *Fbxw7*$^{f/f}$ mice were crossed with R26R female mice (16) to introduce the *LacZ* reporter construct for *Cre*-mediated deletion (The Jackson Laboratory). *Stra8-Cre* transgenic mice were also purchased from The Jackson Laboratory. Genotypes of the mice were examined by PCR with the primers listed in Table S3.

Transplantation. For transplantation, testis cells were dissociated into single-cell suspensions by a two-step enzymatic digestion using collagenase type IV and trypsin (Sigma), as described previously (35). GS cells were incubated with 0.25% trypsin to obtain single-cell suspensions. The donor cells were transplanted into seminiferous tubules of W mice (Japan SLC) through the efferent duct. Approximately 4 μL could be introduced into each testis, which filled 75–85% of the seminiferous tubules.

The Institutional Animal Care and Use Committee of Kyoto University approved all animal experimentation protocols. Further details of procedures are described in the *SI Materials and Methods*.

ACKNOWLEDGMENTS. We thank Ms. Y. Ogata for technical assistance. This research was supported by the government of Japan through its "Funding Program for Next Generation World-Leading Researchers," the Japan Science and Technology Agency (Core Research for Evolutionary Science and Technology, Precursory Research for Embryonic Science and Technology), the Mochida Memorial Foundation for Medical and Pharmaceutical Research, the Takeda Science Foundation, the Uehara Memorial Foundation, and the Ministry of Education, Culture, Sports, Science, and Technology, Japan.

1. de Rooij DG, Russell LD (2000) All you wanted to know about spermatogonia but were afraid to ask. *J Androl* 21(6):776–798.
2. Meistrich ML, van Beek MEAB (1993) Cell and molecular biology of the testis. *Spermatogonial Stem Cells*, eds Desjardins C, Ewing LL (Oxford Univ Press, New York), pp 266–295.
3. Meng X, et al. (2000) Regulation of cell fate decision of undifferentiated spermatogonia by GDNF. *Science* 287(5457):1489–1493.
4. Tegelenbosch RAJ, de Rooij DG (1993) A quantitative study of spermatogonial multiplication and stem cell renewal in the C3H/101 F1 hybrid mouse. *Mutat Res* 290(2):193–200.
5. Brinster RL, Zimmermann JW (1994) Spermatogenesis following male germ-cell transplantation. *Proc Natl Acad Sci USA* 91(24):11298–11302.
6. Kanatsu-Shinohara M, et al. (2003) Long-term proliferation in culture and germline transmission of mouse male germline stem cells. *Biol Reprod* 69(2):612–616.
7. Lee J, et al. (2009) Genetic reconstruction of mouse spermatogonial stem cell self-renewal in vitro by Ras-cyclin D2 activation. *Cell Stem Cell* 5(1):76–86.
8. Ishii K, Kanatsu-Shinohara M, Toyokuni S, Shinohara T (2012) FGF2 mediates mouse spermatogonial stem cell self-renewal via upregulation of Etv5 and Bcl6b through MAP2K1 activation. *Development* 139(10):1734–1743.
9. Lee J, et al. (2007) Akt mediates self-renewal division of mouse spermatogonial stem cells. *Development* 134(10):1853–1859.
10. Oatley JM, Avarbock MR, Brinster RL (2007) Glial cell line-derived neurotrophic factor regulation of genes essential for self-renewal of mouse spermatogonial stem cells is dependent on Src family kinase signaling. *J Biol Chem* 282(35):25842–25851.
11. Oatley JM, Avarbock MR, Telaranta AI, Fearon DT, Brinster RL (2006) Identifying genes important for spermatogonial stem cell self-renewal and survival. *Proc Natl Acad Sci USA* 103(25):9524–9529.
12. Welcker M, Clurman BE (2008) FBW7 ubiquitin ligase: A tumour suppressor at the crossroads of cell division, growth and differentiation. *Nat Rev Cancer* 8(2):83–93.
13. Pashkova N, et al. (2010) WD40 repeat propellers define a ubiquitin-binding domain that regulates turnover of F box proteins. *Mol Cell* 40(3):433–443.
14. Min S-H, et al. (2012) Negative regulation of the stability and tumor suppressor function of Fbw7 by the Pin1 prolyl isomerase. *Mol Cell* 46(6):771–783.
15. Sadate-Ngatchou PI, Payne CJ, Dearth AT, Braun RE (2008) Cre recombinase activity specific to postnatal, premeiotic male germ cells in transgenic mice. *Genesis* 46(12):738–742.
16. Soriano P (1999) Generalized lacZ expression with the ROSA26 Cre reporter strain. *Nat Genet* 21(1):70–71.
17. Atchison FW, Means AR (2003) Spermatogonial depletion in adult Pin1-deficient mice. *Biol Reprod* 69(6):1989–1997.
18. Hobbs RM, Seandel M, Falciatori I, Rafii S, Pandolfi PP (2010) Plzf regulates germline progenitor self-renewal by opposing mTORC1. *Cell* 142(3):468–479.
19. Geng Y, et al. (2003) Cyclin E ablation in the mouse. *Cell* 114(4):431–443.
20. Laurenti E, et al. (2008) Hematopoietic stem cell function and survival depend on c-Myc and N-Myc activity. *Cell Stem Cell* 3(6):611–624.
21. Babaei-Jadidi R, et al. (2011) FBXW7 influences murine intestinal homeostasis and cancer, targeting Notch, Jun, and DEK for degradation. *J Exp Med* 208(2):295–312.
22. Hoeck JD, et al. (2010) Fbw7 controls neural stem cell differentiation and progenitor apoptosis via Notch and c-Jun. *Nat Neurosci* 13(11):1365–1372.
23. Matsumoto A, et al. (2011) Fbxw7-dependent degradation of Notch is required for control of "stemness" and neuronal-glial differentiation in neural stem cells. *J Biol Chem* 286(15):13754–13764.
24. Matsuoka S, et al. (2008) Fbxw7 acts as a critical fail-safe against premature loss of hematopoietic stem cells and development of T-ALL. *Genes Dev* 22(8):986–991.
25. Sancho R, et al. (2010) F-box and WD repeat domain-containing 7 regulates intestinal cell lineage commitment and is a haploinsufficient tumor suppressor. *Gastroenterology* 139(3):929–941.
26. Ruzinova MB, Benezra R (2003) Id proteins in development, cell cycle and cancer. *Trends Cell Biol* 13(8):410–418.
27. Shinohara T, Orwig KE, Avarbock MR, Brinster RL (2001) Remodeling of the postnatal mouse testis is accompanied by dramatic changes in stem cell number and niche accessibility. *Proc Natl Acad Sci USA* 98(11):6186–6191.
28. Ishii K, Kanatsu-Shinohara M, Shinohara T (2014) Cell-cycle-dependent colonization of mouse spermatogonial stem cells after transplantation into seminiferous tubules. *J Reprod Dev* 60(1):37–46.
29. Kanatsu-Shinohara M, Takashima S, Shinohara T (2010) Transmission distortion by loss of p21 or p27 cyclin-dependent kinase inhibitors following competitive spermatogonial transplantation. *Proc Natl Acad Sci USA* 107(14):6210–6215.
30. Bruscoli S, et al. (2012) Long glucocorticoid-induced leucine zipper (L-GILZ) protein interacts with ras protein pathway and contributes to spermatogenesis control. *J Biol Chem* 287(2):1242–1251.
31. Suzuki H, et al. (2012) SOHLH1 and SOHLH2 coordinate spermatogonial differentiation. *Dev Biol* 361(2):301–312.
32. Eilers M, Eisenman RN (2008) Myc's broad reach. *Genes Dev* 22(20):2755–2766.
33. Braydich-Stolle L, Kostereva N, Dym M, Hofmann M-C (2007) Role of Src family kinases and N-Myc in spermatogonial stem cell proliferation. *Dev Biol* 304(1):34–45.
34. Onoyama I, et al. (2007) Conditional inactivation of Fbxw7 impairs cell-cycle exit during T cell differentiation and results in lymphomatogenesis. *J Exp Med* 204(12):2875–2888.
35. Ogawa T, Aréchaga JM, Avarbock MR, Brinster RL (1997) Transplantation of testis germinal cells into mouse seminiferous tubules. *Int J Dev Biol* 41(1):111–122.

Annals of Oncology Advance Access published March 16, 2015

original article

Annals of Oncology 00: 1–8, 2015
doi:10.1093/annonc/mdv034

The *AURKA/TPX2* axis drives colon tumorigenesis cooperatively with *MYC*

Y. Takahashi[1,2,†], P. Sheridan[3,†], A. Niida[3,†], G. Sawada[1,2], R. Uchi[1], H. Mizuno[4], J. Kurashige[1], K. Sugimachi[1], S. Sasaki[5], Y. Shimada[6], K. Hase[7], M. Kusunoki[8], S. Kudo[9], M. Watanabe[10], K. Yamada[11], K. Sugihara[12], H. Yamamoto[2], A. Suzuki[13], Y. Doki[2], S. Miyano[3], M. Mori[2] & K. Mimori[1*]

[1]*Department of Surgery, Kyushu University Beppu Hospital, Beppu;* [2]*Department of Gastroenterological Surgery, Graduate School of Medicine, Osaka University, Suita;* [3]*Laboratory of DNA Information Analysis, Human Genome Center, Institute of Medical Science, University of Tokyo, Tokyo;* [4]*Department of Discovery Research, Kamakura Research Laboratories, Chugai Pharmaceutical Co., Ltd, Kamakura;* [5]*Department of Surgery, Omori Red Cross Hospital, Tokyo;* [6]*Division of Gastrointestinal Oncology, National Cancer Center Hospital, Tokyo;* [7]*Department of Surgery, National Defense Medical College, Tokorozawa;* [8]*Department of Surgery, Mie University, Tsu;* [9]*Digestive Disease Center, Showa University Northern Yokohama Hospital, Yokohama;* [10]*Department of Surgery, Kitasato University, Sagamihara;* [11]*Department of Surgery, Takano Hospital, Kumamoto;* [12]*Department of Surgery, Tokyo Medical and Dental University, Tokyo;* [13]*Division of Cancer Genetics, Medical Institute of Bioregulation, Kyushu University, Fukuoka, Japan*

Received 22 July 2014; revised 18 December 2014 and 30 December 2014; accepted 15 January 2015

Background: The *MYC* oncogene has long been established as a central driver in many types of human cancers including colorectal cancer. However, the realization of *MYC*-targeting therapies remains elusive; as a result, synthetic lethal therapeutic approaches are alternatively being explored. A synthetic lethal therapeutic approach aims to kill *MYC*-driven tumors by targeting a certain co-regulator on the *MYC* pathway.

Patients and methods: We analyzed copy number and expression profiles from 130 colorectal cancer tumors together with publicly available datasets to identify co-regulators on the *MYC* pathway. Candidates were functionally tested by *in vitro* assays using colorectal cancer and normal fibroblast cell lines. Additionally, survival analyses were carried out on another 159 colorectal cancer patients and public datasets.

Results: Our *in silico* screening identified two *MYC* co-regulator candidates, *AURKA* and *TPX2,* which are interacting mitotic regulators located on chromosome 20q. We found the two candidates showed frequent co-amplification with the *MYC* locus while expression levels of *MYC* and the two genes were positively correlated with those of *MYC* downstream target genes across multiple cancer types. *In vitro*, the aberrant expression of *MYC*, *AURKA* and *TPX2* resulted in more aggressive anchorage-independent growth in normal fibroblast cells. Furthermore, knockdown of *AURKA* or *TPX2*, or treatment with an *AURKA*-specific inhibitor effectively suppressed the proliferation of *MYC*-expressing colorectal cancer cells. Additionally, combined high expression of *MYC*, *AURKA* and *TPX2* proved to be a poor prognostic indicator of colorectal cancer patient survival.

Conclusions: Through bioinformatic analyses and experiments, we proposed *TPX2* and *AURKA* as novel co-regulators on the *MYC* pathway. Inhibiting the *AURKA/TPX2* axis would be a novel synthetic lethal therapeutic approach for *MYC*-driven cancers.

Key words: MYC, AURKA, TPX2, synthetic lethality, co-amplification

introduction

The *MYC* oncogene residing on chromosome 8q24 has been established as a central driver in various types of human cancers. Amplification of the *MYC* locus is frequently observed in many types of cancers and is associated with poor prognosis [1–3]. Inhibition of *MYC* is an attractive pharmacological approach for *MYC*-driven tumors. However, *MYC*-targeting therapies remain to be realized, due to difficulties in designing small-molecule drugs and anticipated side-effects incurred by inhibiting normal proliferating tissues [4]. To overcome these difficulties, synthetic lethal therapeutic approaches are currently being explored; we could selectively kill *MYC*-driven tumors by targeting a certain co-regulator on the *MYC* pathway [5].

Correspondence to: Prof. Koshi Mimori, Department of Surgery, Beppu Hospital, Kyushu University, 4546, Tsurumihara, Beppu 874-0838, Japan. Tel: +81-977-27-1650; Fax: +81-977-27-1651; E-mail: kmimori@beppu.kyushu-u.ac.jp

†These authors contributed equally to this work.

In this study, we bioinformatically searched gene expression and copy number profiles of colorectal and other types of cancers for co-regulators on the MYC pathway, yielding Aurora A kinase (*AURKA*) and Targeting protein for Xklp2 (*TPX2*) as candidates. Our experiments verified the two genes cooperatively act with *MYC* in colorectal cancer cells and revealed that an *AURKA* inhibitor was effective for *MYC*-driven colorectal cancer, suggesting a novel synthetic lethal therapeutic approach.

materials and methods

sample collection and extraction of DNA and RNA

We used a total of 289 colorectal cancer samples, 130 of which (set 1) were used as pure cancer tissues separated by laser microdissection (all cases were used for microarray analyses), and 159 (set 2) were used in bulk for quantitative reverse transcription PCR. All patients underwent resection of the primary tumor at Kyushu University Beppu Hospital and affiliated hospitals between 1992 and 2007. Full informed consent was obtained from all individuals according to local ethical review board approval. The follow-up period in set 1 ranged from 0.1 months to 3.2 years with a mean of 2.1 years; the follow-up period in set 2 ranged from 0.1 to 12.3 years, with a mean of 3.8 years. Resected tissues were processed as previously described [6]. All sample data, including survival information, were obtained from the clinical and pathologic records.

in vitro analysis and microarray analysis

Detailed information is reported in supplementary Data, available at *Annals of Oncology* online.

analysis of public database

Detailed information is reported in supplementary Data, available at *Annals of Oncology* online.

EEM analysis

Extraction of expression modules (EEM) was developed to extract expression modules from a given expression dataset. In this framework, a gene set whose members behave coherently in the dataset is referred to as an expression module. In contrast to unsupervised clustering approaches, EEM starts from a seed gene set that is associated with some biological function (e.g. genes with a common GO term or target gene candidates of a common transcription factor). EEM first tests expression coherence of the seed gene set in the expression dataset. If correlation is statistically significant, EEM extracts a coherent subset of the gene set as an expression module, and the geometric center of expression profiles of module members is obtained as an activity profile of the expression module. The methodological detail has previously been described by Niida et al. [7, 8]. In this study, to extract a *MYC* activity-associated expression module, the 'NEVINS_MYC_UP' gene set was prepared by using the expression array data [9] and was used as the seed gene set.

multiple linear regression analysis

As described below, *MYC* expression alone did not satisfactorily account for the variations in *MYC* activity profiles of the colorectal cancer clinical gene expression microarray data. In order to account for this discrepancy, we carried out a separate multiple linear regression analysis for each gene to model the relationship between the *MYC* activity profile (response variable) and the expression profiles of *MYC* together with the given gene under investigation (explanatory variables). The model interpretation is straightforward: the *P* value of the regression coefficient for a given gene provides a measure of the amount of variation in the *MYC* activity profile that was explained by that gene when controlling for the effect of *MYC* expression. From there, a list of candidate genes, that is, genes that were potential co-regulators of *MYC* activity, was obtained simply by taking all genes with *P* values below a certain cutoff value.

results

in silico screening for MYC co-regulators

First, we analyzed the expression profiles of *MYC* downstream target genes (hereafter, referred to as the *MYC* module activity) using the EEM algorithm [7, 8]. We found that *MYC* mRNA expression correlates with the *MYC* module activity on our mRNA expression array data of 130 colorectal cancer clinical samples. However, a substantial fraction of the variation of the *MYC* module activity is not explained only by *MYC* mRNA expression levels (supplementary Figure S1, available at *Annals of Oncology* online), suggesting that that *MYC* activity in *MYC*-driven cancer cells is also dependent on other factors.

We also carried out array-CGH analysis for the same case set; in our data, the *MYC* locus 8q24 is frequently amplified and the amplification leads to *MYC* overexpression in the mRNA level, consistently with previous studies [10]. Moreover, we observed co-amplification between 8q24 and 20q (Figure 1A), whose amplification is also reported to be a significant genomic event in cancer tissues [11, 12]. Notably, we confirmed that this co-amplification occurs in various types of cancers by analyzing publicly available copy number data (Figure 1B and C). Based on these observations, we hypothesized that some driver genes functionally interacting with *MYC* reside on 20q and co-amplification between 8q24 and 20q are evolutionally selected due to the functional interaction driving carcinogenesis.

Based on this hypothesis, we attempted to find unknown factors on 20q that regulate *MYC* module activity cooperatively with *MYC*. We carried out multiple regression analysis in which the *MYC* module activity is a dependent variable while mRNA expression levels of *MYC* and each gene on 20q are independent variables. Consequently, we found that two genes interacting with each other, *AURKA* and *TPX2*, as candidates for *MYC* module co-regulator (Figure 1D and E and supplementary Table S1, available at *Annals of Oncology* online). *AURKA* is known to regulate cell division by phosphorylating multiple downstream targets in the mitotic apparatus and the full activation and correct mitotic localization of *AURKA* require its interaction with the spindle regulator *TPX2* [13, 14]. Expression profiles of *AURKA* and *TPX2* are strongly correlated (supplementary Figure S2, available at *Annals of Oncology* online), and the *MYC* module activity tended to increase when *MYC* high expression was accompanied by the high expression of *AURKA* and *TPX2* (Figure 1D and E). We validated this relationship on multiple public expression datasets covering multiple cancer types. In our meta-analysis of the public datasets, *AURKA* and *TPX2* also scored one of the most significant *P* values (Figure 1F, supplementary Figure S3A and B, Tables S2 and S3, available at *Annals of Oncology* online). We also found that copy number and expression profiles of *AURKA*/*TPX2* are correlated with each other as well as those of *MYC* in our colorectal cancer dataset (supplementary Figure S2, available at *Annals of Oncology* online). Taken together, we predicted that *AURKA* and *TPX2*, which are co-amplified and co-overexpressed with *MYC*, act as cooperative driver genes in the *MYC* pathway.

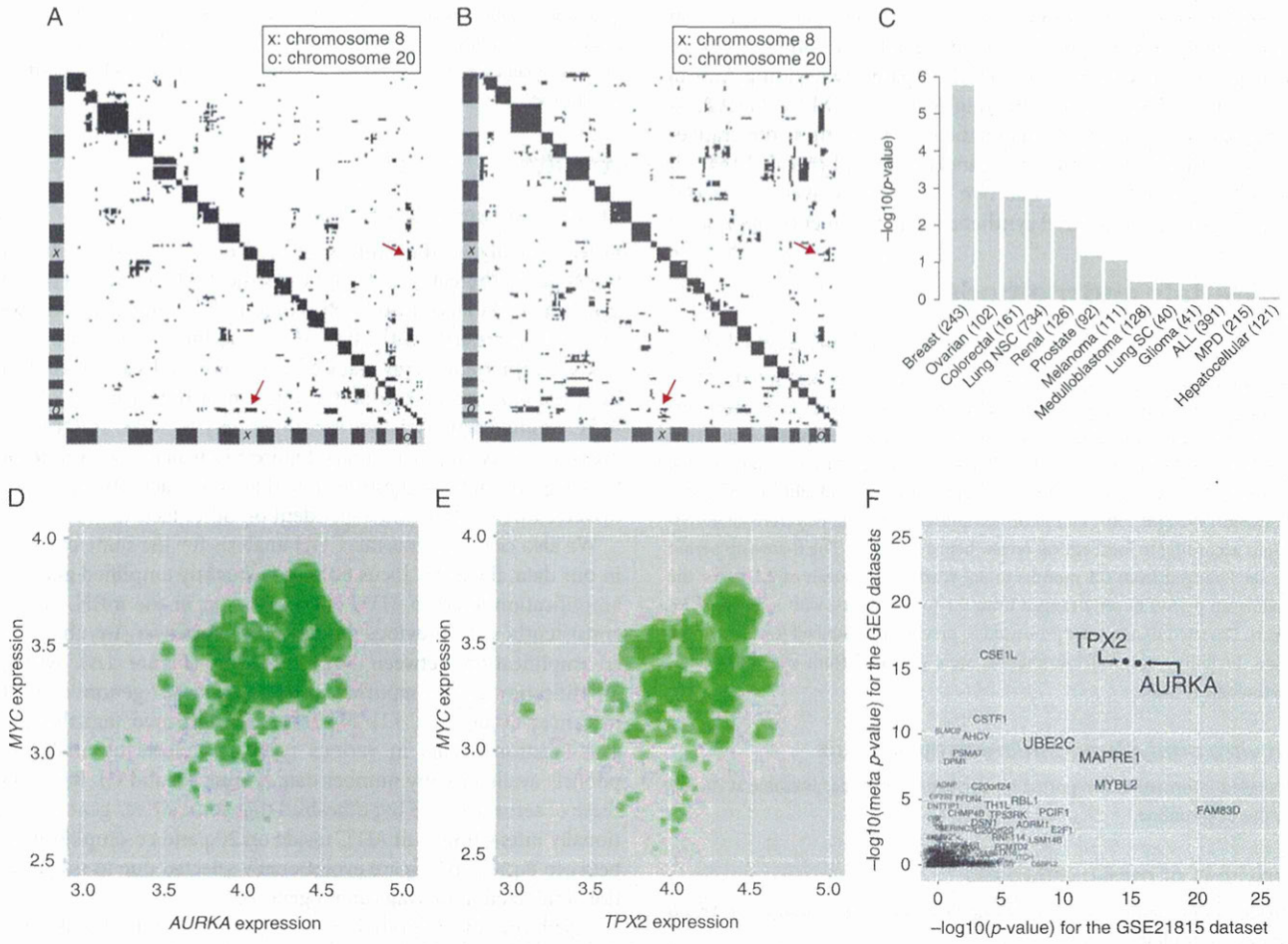

Figure 1. Bioinformatic analyses to predict *AURKA* and *TPX2* as co-regulators of *MYC* activity. (A) Copy number correlation profiles were calculated for array-CGH data of 130 colorectal cancer cases. The vertical and transverse axes of the visualized correlation indicate chromosomal regions and black regions in the matrix represent pairs scoring *P* values $<10^{-5}$. 'x' indicates chromosome 8 and 'o' indicates chromosome 20. The copy numbers of chromosomes 8q24 and 20q were positively correlated in this case set (arrow). (B) Copy number correlation was also assessed with publicly available data (Tumorscape database) consisting of about 3000 cases containing various cancer types, and shown as (A). (C) Analysis of co-amplification of chromosomes 8q24 and 20q for each type of cancers. Correlation of copy number profiles between 8q24 and 20q was calculated for in each type of cancer in the dataset used in (B) The transverse axis indicates *P* value (−log10 [*P* value]) for co-amplification of 8q24 and 20q and numerals in parentheses indicate number of case sets for each cancer type. (D and E) Balloon plots showing *MYC* module activity and expression levels of the potential regulators. Each axis represents expression levels of *MYC* and *AURKA* (D), or *TPX2* (E) and the size of each balloon indicates the level of *MYC* module activity in our colorectal cancer dataset. (F) Multiple regression *P* values: our colorectal cancer datasets (GSE21815) and the public datasets. For the expression level of each gene on 20q, multiple regression analysis is carried out on *MYC* module activity together with the expression level of *MYC*. The transverse axis represents *P* values for our datasets while the vertical axis represents *P* values from meta-analysis of the public datasets.

cooperative function of MYC, AURKA and TPX2 on anchorage-independent growth

Based on our prediction, we examined functional interactions between *MYC* and the two 20q genes in carcinogenesis. The impact of aberrant expression of the three genes was evaluated on a normal fibroblast cell line (KMST-6). We used KMST-6 cells that stably expressed each of the three genes either alone or in combination (Figure 2A). Each of *MYC*, *AURKA* and *TPX2* expression promoted anchorage-independent growth in KMST-6 cells. Furthermore, combinational overexpression of these three genes induces more aggressive phenotypes (Figure 2B and C), supporting a cooperative effect between *MYC* and 20q genes for tumorigenesis.

crucial function of AURKA/TPX2 in MYC-dependent colorectal cancer cells

Next, we examined the functional interactions between *MYC* and *AURKA/TPX2* in colorectal cancer cell lines. We analyzed the cell growth inhibition by knockdown of *AURKA/TPX2* using siRNA on two colorectal cancer cell lines with different *MYC* expression level and different 8q and 20q copy number profile [data from Cancer Cell Line Encyclopedia (CCLE) database [15]; supplementary Figure S4, available at *Annals of Oncology* online]: HCT-116 with aberrant *MYC* expression and DLD-1 without aberrant *MYC* expression (Figure 3A).

We observed that knockdown of *TPX2* more strongly suppressed cell proliferation in HCT-116 cells than in DLD-1 cells,